High-Throughput Spectroscopic Imaging Applied to Permeation Through the Skin

JEAN-MICHEL ANDANSON, K. L. ANDREW CHAN, and SERGEI G. KAZARIAN*

Department of Chemical Engineering, Imperial College London, South Kensington Campus, London, SW7 2AZ, United Kingdom

Infrared (IR) spectroscopy has been successfully applied to study the permeation of substances through human skin in a high-throughput manner. The sample of skin was placed on the measuring surface of an attenuated total reflection (ATR) crystal and was divided into several areas. These areas were separated using a specially designed grid created on the surface of the skin and each area was subjected to a different combination of permeant and enhancer. ATR Fourier transform infrared (FT-IR) imaging was applied to measure the permeation of 12 liquid samples through a piece of skin smaller than 5 cm^2. This work demonstrated that, using the ATR-FT-IR imaging method, it is possible to measure and directly compare the transdermal processes of several permeants under identical conditions.

Index Headings: **High throughput; Drugs; Human skin; Diffusion; Stratum corneum; Imaging; Attenuated total reflection; Fourier transform infrared spectroscopy; ATR-FT-IR imaging.**

INTRODUCTION

Human skin is a natural efficient barrier that protects our body from the physically and chemically hostile environment[1] while maintaining hydration inside the body. The epidermis, in particular the stratum corneum, which is the outmost layer of the skin, provides most of the barrier function. This effective barrier function often makes drug delivery difficult and reduces the effectiveness of some of the topical treatments. Different formulations of pharmaceutical creams have been developed to enhance the effectiveness of drug permeation through the skin. However, the accuracy of the comparison of the performance between different formulations relies on the repeatability of the results. Infrared (IR) spectroscopy is a powerful technique that has been employed to study the diffusion of drugs through the skin.[2–4] However, the measurements of the permeability within the intra and/or inter-subject tests have shown significant variability, making it difficult to compare the results.[5] A high-throughput method is required for large scale studies to obtain statistically significant results.[6,7]

Attenuated total reflection Fourier transform infrared (ATR-FT-IR) spectroscopy, while having the advantages of minimal sample preparation and being appropriate for strongly absorbing materials, is found to be suitable for skin permeation studies.[8–10] The combination of the ATR-FT-IR method with a focal plane array (FPA) detector allows ATR-FT-IR images to be captured in a relatively short time (1 second per scan). This capability has been utilized to study skin hydration under controlled humidity.[11] Previous studies have also demonstrated that it is possible to perform high-throughput studies of ~40 pharmaceutical formulations simultaneously.[12] With the development of the ATR accessory with expanded optics, screening of up to 160 formulations in one image snapshot has been demonstrated.[13,14]

In this work, we extended the application of the ATR accessory with the expanded field of view to study drug permeation through human skin in a high-throughput manner. This new approach provides the opportunity to measure drug permeation from several formulations simultaneously for a direct comparison. It should be noted that the ATR spectroscopic approach does not reflect the situation for diffusion through the skin. The usual approach to studying transdermal permeation is using Franz type diffusion cells where the solution is placed on top of the skin tissue and permeation is measured in a receptor solution, which is an infinite sink. In our previous studies we used Franz diffusion cells but the analysis of skin samples was done *ex situ* using a tape-stripping method.[4] Clearly, having the ATR crystal on one side of the skin sample (as in our ATR imaging approach) would affect the diffusion profile. Nevertheless, for the purpose of direct comparison of different formulations, the *in situ* imaging approach introduced here has much potential.

EXPERIMENTAL METHODS

The sample was an abdominal cadaver skin obtained with appropriate ethical approval and was prepared using the procedure principles described previously.[15] The thickness of the dry sample of skin was approximately 25 μm, which changes to approximately 50 μm for the wetted skin sample.

Poly(dimethylsiloxane) PDMS (Sylgard 184) elastomer kit, isopropyl-myristate (IPM, 98% pure), poly(ethylene glycol) (PEG) 400, and 4-cyanophenol (95% pure) were purchased from Sigma. DMSO was obtained from Prolabo and the ethanol used was analytical grade (99.7%). 4-Cyanophenol is one of the model substances, which has been used before to study permeation through the skin.[16–18]

Fourier transform infrared images were measured by simultaneously capturing 4096 spectra using a 64 × 64 FPA detector and a continuous scan FT-IR spectrometer operating at 4 cm^{-1} spectral resolution with 64 scans. Each spectrum corresponds to the chemical components at a specific position on the surface of the ATR crystal such that chemical images can be built from the spectral information. The concept of ATR imaging is patented by Varian.[19] By plotting the integrated absorbance of a specific spectral band in the mid-infrared spectrum, it is possible to obtain the distribution and concentrations of a particular compound in different parts of the whole imaged area. The principle of FT-IR imaging has already been explained in detail in previous studies.[4,20–22]

The ATR accessory with an expanded field of view (ATR-ExFoV), which includes a large inverted pyramid ZnSe crystal with an angle of incidence of 45°, two expanding lenses, and four plane mirrors, was used. The measuring surface of the crystal has dimensions of 19 mm × 26 mm; further details of

Received 29 December 2008; accepted 11 February 2009.

* Author to whom correspondence should be sent. E-mail: s.kazarian@imperial.ac.uk.

0003-7028/09/6305-0512$2.00/0

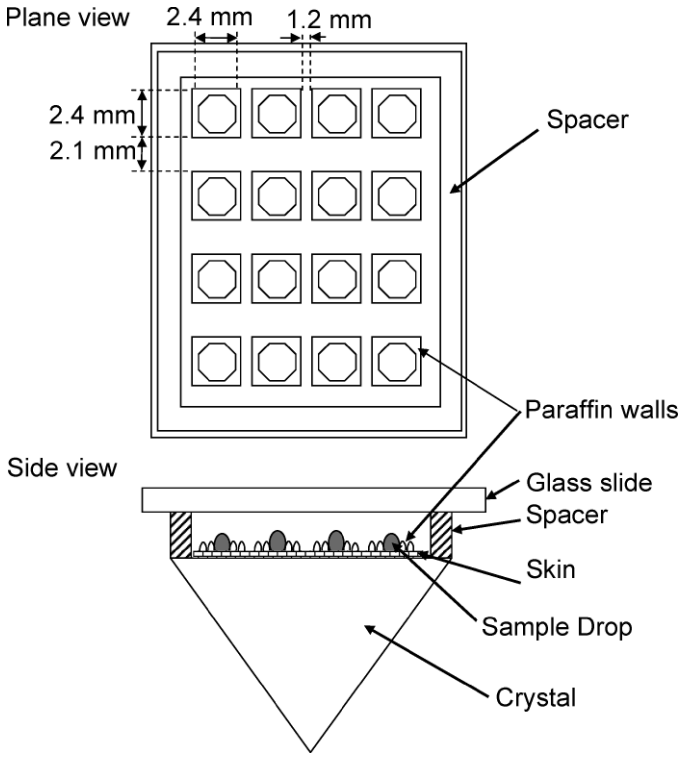

FIG. 1. (**Top**) Schematic diagram showing the location of the paraffin grid on the ATR crystal with detailed dimensions of the well. (**Bottom**) Schematic presentation of the setup of the experiment with skin during measurement.

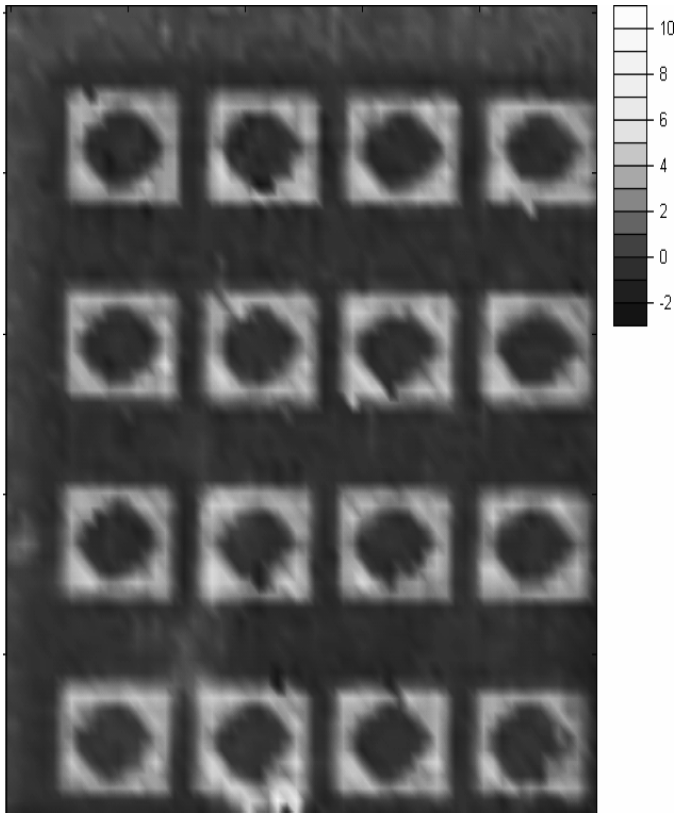

FIG. 2. ATR-FT-IR imaging showing the location of the paraffin grid (or well) printed directly onto the measuring surface. Imaging area is ~22 mm × 16 mm.

this ATR accessory are described in a previous work.[23] The total image size of this system has been determined to be 16 mm by 22 mm, which gives a pixel size resolution approximately 0.24 × 0.34 mm^2.

The micro-droplet-on-demand device (AutoDrop®, Micro-Drop) consists of a dispensing control unit with heated dispensing heads, a built-in computer, an *xyz* positioning system, and a controlling unit. Paraffin was heated to 85 °C during printing with parameters adjusted such that each drop of paraffin has a diameter of ~0.05 mm.

Four saturated model solutions of 4-cyanophenol were prepared by mixing excess 4-cyanophenol with 70 wt. % water, 20 wt. % PEG 400, and 10 wt. % ethanol, IPM, or DMSO in solutions 1 (S1), 2 (S2), and 4 (S4), respectively, and 5 wt. % ethanol and 5 wt. % DMSO in solution 3 (S3).

RESULTS AND DISCUSSION

For a high-throughput study, multiple samples are deposited onto a relatively large piece of skin such that the permeation process of each sample can be monitored simultaneously. To obtain the highest number of formulations to be studied in one sample, ideally the different formulations should be applied as close to each other as possible with the applied solution occupying an imaged area of 1 pixel (~0.24 mm × 0.34 mm in the used accessory). Considering that a minimum separation of 1 pixel is required between each sample due to the limitations of the spatial resolution, the theoretical maximum number of formulations that may be studied was estimated to be around 1024 for a 4096 pixels detector.[13] However, the solution was not directly applied to the measuring surface of the ATR crystal but rather to the skin placed on the surface of the ATR. A greater minimal distance of separation between samples would be needed because the solute is expected to diffuse in a more complex manner rather than just perpendicular to the surface of the skin. Thus, apart from diffraction effects, separation between solutions is needed to prevent physical cross-contamination on the surface of the skin. Previous studies[12–14,24] rely on the spaces between samples and the surface tension of each solution to maintain the separation. However, this approach is only suitable for experiments with a small amount of solution and solutions that do not spread after deposition. For the permeation experiments, there should be excess solution in order to minimize changes in the solution during the permeation process. The relatively large amount of solution that is required for deposition makes it impossible to separate samples in a confined area if the separation only relies on the surface tension. A physical wall must be constructed for this purpose to confine each solution. Solid paraffin has been considered as one of the possible materials to build such confining walls.

Experiment Without Skin. To characterize the paraffin grid and ensure that it does not delaminate after deposition, paraffin wells made by a series of small paraffin drops were printed directly on the surface of the ZnSe crystal without the skin. The dispenser was set to dispense micro-drops of wax assembled together to create walls. The thickness of the wax wall is determined by the diameter of each paraffin drop, ~0.05 mm, which is below the resolution of the image obtained using this ATR accessory. Considering the possible spectral and physical contamination between solutions and the volume of the solution, 2.4 mm (approximately the size of 10 image pixels) is thought to be a reasonable diameter for each well. A

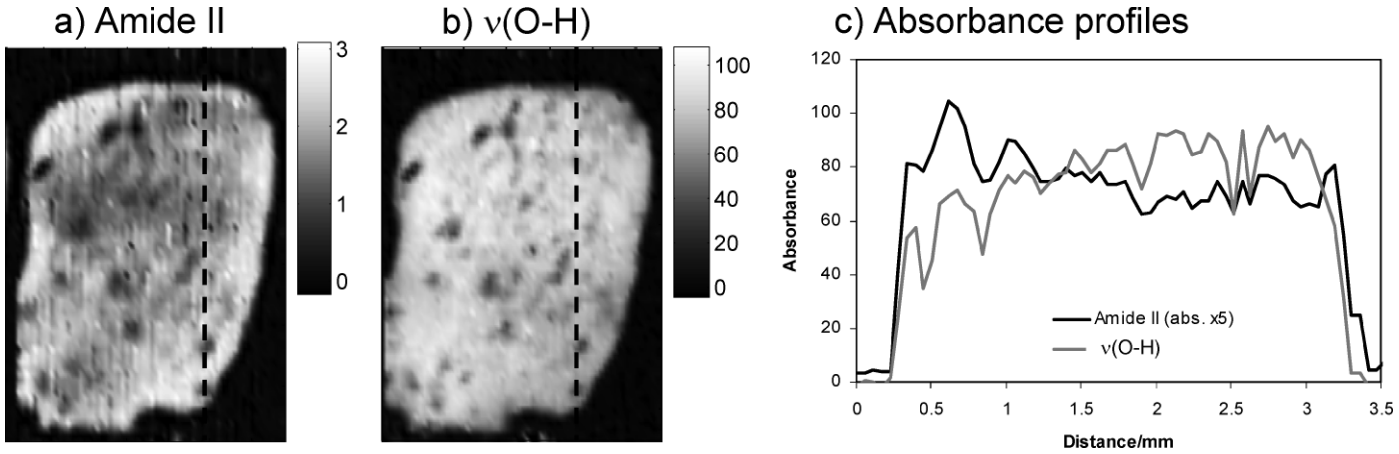

FIG. 3. (**a**) ATR-FT-IR image of protein distribution based on the amide II bands. (**b**) ATR-FT-IR image of water distribution based on the ν(O–H) band. (**c**) Absorbance profiles extracted along the line shown in Figs. 3a and 3b. Imaging area is ~22 mm × 16 mm.

minimum separation of 1.2 mm (0.6 mm from the edge of each well, ~10 times the thickness of skin) is also used. The dimensions and separations between wells are summarized in the diagram in Fig. 1a.

An octagonal shape was used instead of square because the solution tended to leak at the relatively sharp corners (90° for a square compared to 135° for an octagon), limiting the amount of solution that can be held in each well. The results of the deposition of paraffin on the surface of the diamond using the MicroDrop system are shown in Fig. 2. The strong and continuous absorbance of the paraffin C–H stretching band between 3000 and 2800 cm^{-1} demonstrated that the printed paraffin walls are firmly attached to the ATR crystal surface. Extra lines were added around the paraffin wells to prevent spreading of the solution in case of a small leakage through the inner paraffin walls. It has been found that each well can carry ~4 μL of solution without spillage. This is considered excess solution in relation to the volume of the skin directly underneath the solution (approximately 0.3 μL).

Experiment With Skin. The idea of the sample arrangement for this high-throughput skin permeation study is schematically illustrated in Fig. 1b. The skin is first firmly attached to the measuring surface of the ATR crystal in a similar manner to that described previously.[25] In brief, a piece of wet skin was laid on the top of the crystal before drying at room conditions (~23 °C and 40% RH). The preparation of the sample involved cutting a small, rectangular piece of SC (stored at −20 °C), typically around <5 cm^2. The piece of skin was then defrosted to room temperature and rehydrated by leaving a drop of water on top of the sample (with the internal part of the skin in contact with the water). The skin (thickness with epidermis, ~50 μm) was put on the ZnSe crystal with the epidermal part of the skin in contact with the crystal. The 16 octagons were drawn on the top of the skin by printing heat-liquefied paraffin microdrops to form walls for the confinement of the solution. Finally, 4 μL of different solutions were added manually using a pipette into the "wax wells" before capturing ATR-FT-IR images as a function of time. A 2 mm high PDMS spacer and a glass slide were put on the top of the crystal to enclose the whole system to reduce the evaporation of the sample drops.

While the coverage of the skin on the ATR crystal was good in the beginning, it started to delaminate from the edge when the skin continued to dry. Such a phenomenon was not observed before because previous studies utilized smaller pieces of skin. When the skin was wet, it was fully swollen with water. However, as water evaporated, the edge of the skin tended to dry more quickly than the center of the skin, causing the edge to shrink more than the center. This was observed from the absorbance of amide II bands (between 1580–1480 cm^{-1}), which varied across the skin (Fig. 3a). A complementary image to Fig. 3a has been created wherein the absorbance of water, the ν(O–H) band at 3700–3000 cm^{-1}, is plotted as a map (Fig. 3b). In this region of the spectrum, both the water ν(O–H) band and the protein ν(N–H) band are present. Since the water ν(O–H) band is much stronger than the protein ν(N–H) band, a higher water concentration (hence, greater swelling of the skin by water) would result in a higher overall absorbance in the 3700–3000 cm^{-1} region. Figure 3b demonstrates that the weaker amide II band observed in the center areas was due to a greater swelling of the skin by water. Figure 3c shows the absorbance profiles of the amide II and ν(O–H) bands along the dotted line on Figs. 3a and 3b. The profiles confirm that when the amide II band becomes weaker, the ν(O–H) band becomes stronger.

There are a few black spots that appear on the same area of Figs. 3a and 3b and that appear as valleys in the profiles in Fig. 3c. Spectra extracted in those areas have all shown a reduction in spectral absorbance, which is caused by small air bubbles trapped underneath the skin. Nevertheless, these areas do not interfere with the experiment conducted in this study. At the edge of the skin, the skin is more dehydrated, and hence is less swollen by water, and the absorbance of protein is stronger. Note that this indicates that drying occurs from the outer sides of the sample, rather than from the top layer near the air interface, because of the effectiveness of the stratum corneum in protecting the skin from drying. Due to the shrinkage and delamination at the edges, only 12 out of the 16 octagons were used. Each row of wells was filled with the same solution such that there will be 2–4 repeat measurements for each sample in the same row (S1 to S4 from the top to the bottom of Fig. 3). During the experiment an image was recorded every 10 minutes for 8 hours.

The images for permeation of the 4-cyanophenol through the skin at selected times are shown in Fig. 4a. The images were obtained using the band between 2250 and 2200 cm^{-1},

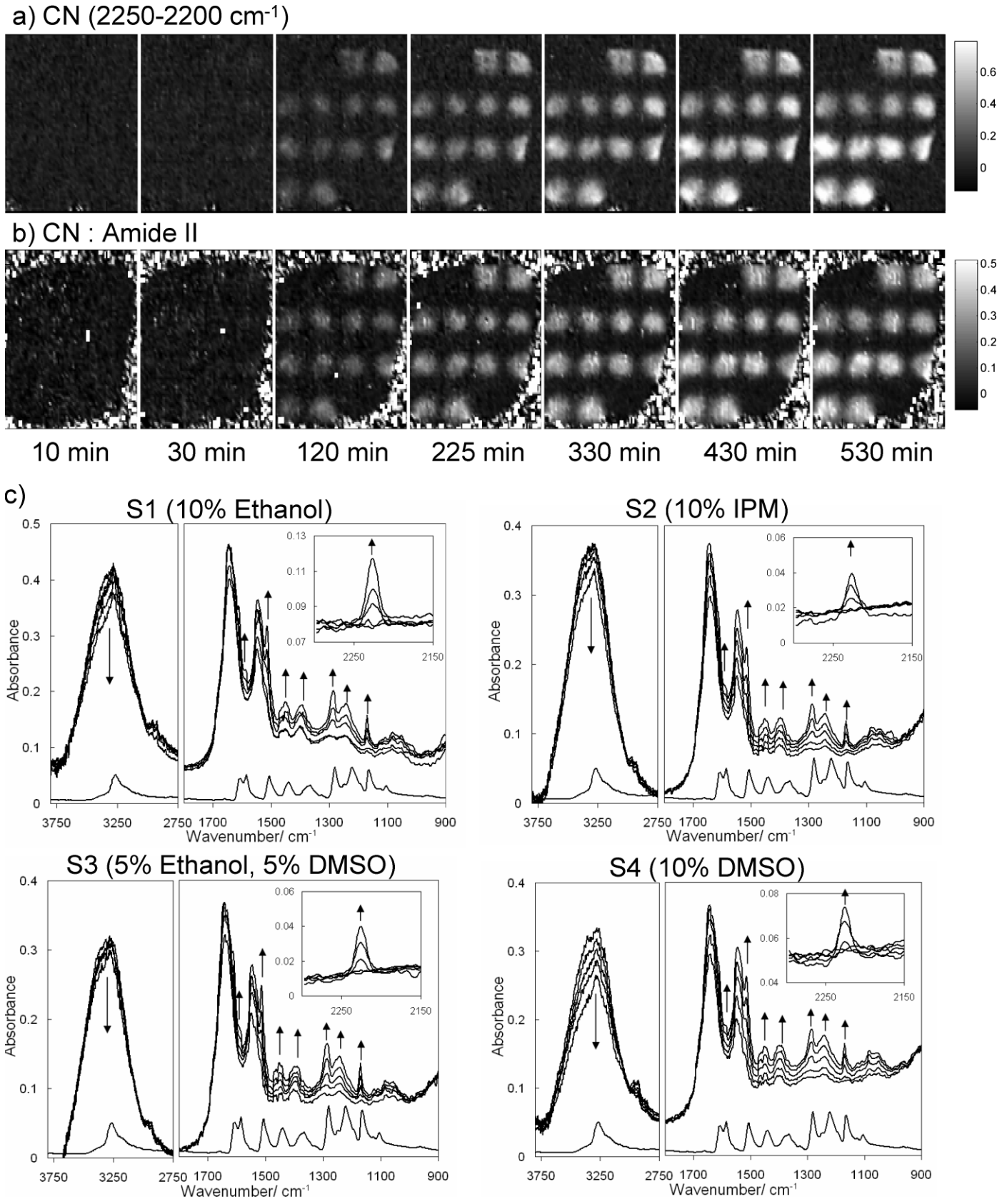

FIG. 4. (**a**) A series of ATR-FT-IR images showing the distribution of 4-cyanophenol based on the absorbance between 2250 and 2000 cm^{-1} measured at different times. (**b**) A series of ATR-FT-IR images based on the CN:amide II band ratio. Images are captured at the time indicated at the bottom of (b). (**c**) Extracted spectra from the areas of skin under different formulations (indicated above each plot) as a function of time. The spectrum of dry powdered cyanophenol is shown at the bottom of each plot. Arrows indicate the direction of the change of spectral features as a function of time. Imaging area is ~22 mm × 16 mm.

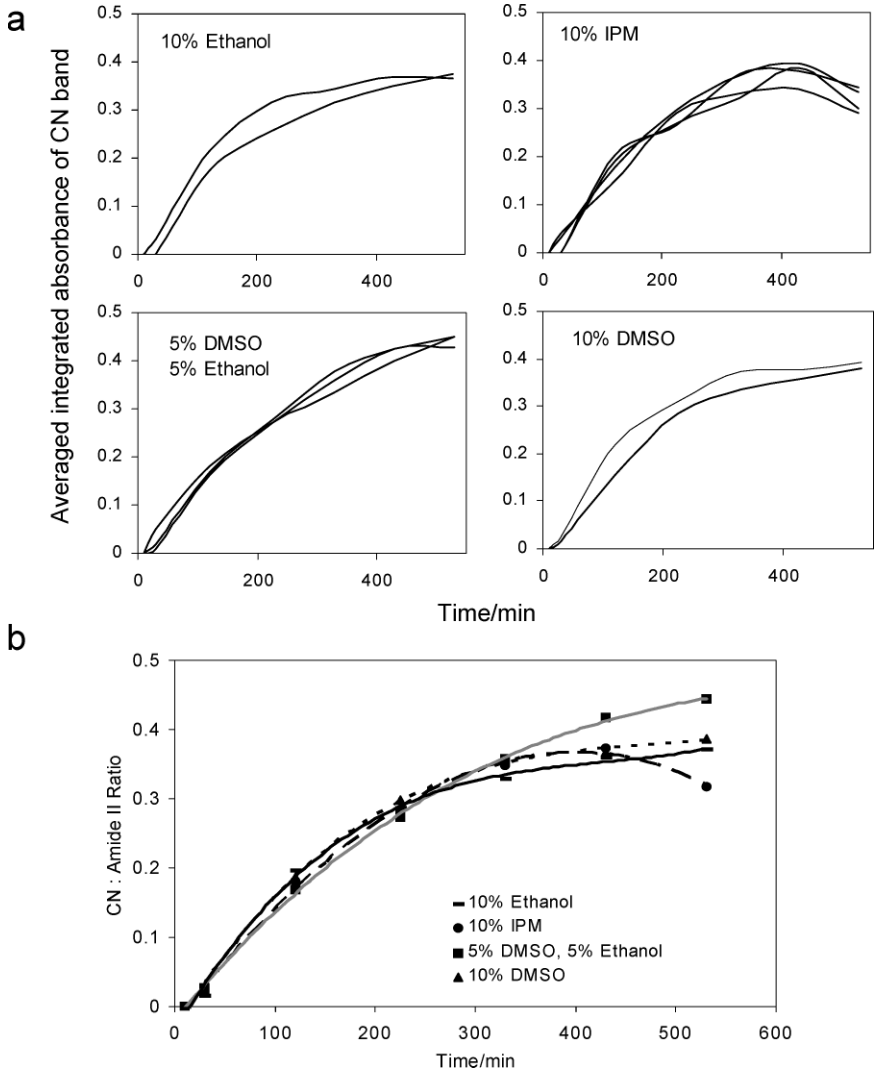

FIG. 5. (**a**) Individual profiles of the CN:amide II absorbance ratio observed in the skin as a function of time for all studied wells. Experiments with wells containing the same formulation (within each row) are plotted in the same graph to demonstrate reproducibility between repeated experiments. (**b**) The average profiles of the CN:amide II absorbance ratio for the different formulations studied.

corresponding to the CN stretching mode vibration. The spectra extracted from areas under the different formulations at various time points (Fig. 4c) showed that apart from the C–N bands (Fig. 4c inset), most of the spectral bands of cyanophenol also increased as a function of time. The spectrum of pure cyanophenol powder was inserted at the bottom of each plot for comparison purposes. A shift in the spectral bands can be observed when comparing the cyanophenol dry powder spectrum to the spectrum of partitioned cyanophenol in skin. It is interesting to note that although different formulations have been used, the spectra extracted from areas under different formulations looked very similar towards the end of the experiment.

Spectral bands of the solvent used were not observed in all formulations (except water bands, which were also present in the skin in the beginning of the experiment). The first appearance of 4-cyanophenol that had diffused through the human epidermis was observed 30 minutes after the application of the solutions on the SC surface. The concentration of 4-cyanophenol continues to increase as a function of time until it reaches equilibrium at 480 minutes. Despite the same formulation being deposited in each row, the 4-cyanophenol concentration appears to vary significantly. In the region where the skin was less hydrated (near the edge of the skin), the 4-cyanophenol concentration was higher because there was less water in the skin. The ratio between the absorbance of the CN band of 4-cyanophenol and the amide II band of protein has been calculated and plotted as images shown in Fig. 4b. The differences in absorbance of the CN band across each row of samples have been removed using this ratio approach. The lack of differences in 4-cyanophenol concentration within each row of samples suggests that the permeation behavior appears to be relatively independent of the hydration level of the skin for the systems studied.

The profiles of the CN:amide II band ratio as a function of exposure time for each well have been extracted and are presented in Fig. 5a. The profiles extracted within each row showed similar trends, hence demonstrating the reproducibility of this approach. The profile was plotted using the averaged absorbance of the CN band extracted from 6–9 pixels (bad pixels are rejected) at the center of each well. It was challenging to achieve good reproducibility with different skin

samples; therefore, it is important to perform the comparative experiment with the same piece of skin. However, an improvement of the homogeneity of the hydration level may be important for other systems. The main challenge was in ensuring a good attachment of the relatively large skin sample to the whole surface of the ATR crystal. This issue needs to be solved to use the approach introduced here as a screening technique. Alternatively, improvement of the homogeneity of the contact and hydration may be achieved by cutting the piece of skin into several smaller pieces and arranging them in an array such that the wax grid could then be printed on top. This can be explored in the future studies.

It is also interesting to note that at the end of the experiment, the amount of 4-cyanophenol per unit amount of skin is higher for S3 than S4 and S1, followed by S2. The average absorbance profiles were compared between each row and the results have been plotted in Fig. 5b. Trend lines have been added as visual aids to demonstrate that the absorption profiles were very similar in the first 330 minutes of the experiment. However, the skin under formulation S3 showed a continued increase in the CN:amide II ratio towards the end of the experiment, while the area under the S1 and S4 formulations showed that the system reached equilibrium towards the end and the S2 solution showed a slight decrease in the last measurement. The results have demonstrated that ethanol and DMSO induced a higher partitioning of cyanophenol in the skin than IPM, while the combination of ethanol and DMSO has the greatest effect on increasing this partitioning effect. It has been reported recently that DMSO may improve the partitioning of cyanophenol into the stratum corneum;[26] DMSO is a known skin-penetration enhancer.[27] It is not clear why the formulation with 10% IPM shows a relative decrease in the concentration of 4-cyanophenol at the end. A possible explanation could be that IPM diffuses more slowly through the skin compared to 4-cyanophenol but when it reaches equilibrium its concentration is sufficient that it replaces some 4-cyanophenol from the bottom layers of the skin.

The experimental results presented here have shown the possibility of studying the permeation of multiple samples through human skin *in situ* using the ATR-FT-IR imaging method with the expanded field of view ATR accessory. The advantage of this approach includes the high-throughput nature of the experiment, reduced variability of conditions (temperature, humidity) between experiments, and miniaturization of sample usage. Currently the number of samples studied in one experiment is limited to the size of the skin that can maintain good contact during the experiment. A greater shrinkage problem is expected for larger pieces of skin. However, this problem may be overcome by sectioning the skin into separate smaller pieces before attaching them onto the ATR crystal.

CONCLUSION

We report the first example of high-throughput studies of transdermal permeation through skin using ATR-FT-IR imaging. The permeation of 12 samples (potentially up to 16 samples with the current setup) has been studied simultaneously. This approach has allowed us to measure and directly compare transdermal processes of several permeants under identical conditions. ATR-FT-IR imaging was applied to measure the permeation of 12 liquid samples on a piece of skin smaller than 5 cm^2. These results show the possibility of studying transdermal permeation of several formulations simultaneously using ATR-FT-IR imaging.

ACKNOWLEDGMENTS

We thank EPSRC for support (grants EP/D502721 and EP/D066859/1) and Prof. J. Hadgraft (London School of Pharmacy) for providing skin samples.

1. A. Williams, *Transdermal and Topical Drug Delivery* (Pharmaceutical Press, London, 2003).
2. M. Hartmann, B. D. Hanh, H. Podhaisky, J. Wensch, J. Bodzenta, S. Wartewig, and R. H. H. Neubert, Analyst (Cambridge, U.K.) **129,** 902 (2004).
3. E. Touitou, V. M. Meidan, and E. Horwitz, J. Control. Release **56,** 7 (1998).
4. M. Boncheva, F. H. Tay, and S. G. Kazarian, J. Biomed. Opt. **13,** 064009 (2008).
5. D. Southwell, B. W. Barry, and R. Woodford, Int. J. Pharm. **18,** 299 (1984).
6. P. Karande, A. Jain, and S. Mitragotri, Nature Biotechnol. **22,** 192 (2004).
7. P. Karande, A. Jain, A. Arora, M. J. Ho, and S. Mitragotri, Eur. J. Pharm. Sci. **31,** 1 (2007).
8. C. Curdy, A. Naik, Y. N. Kalia, I. Alberti, and R. H. Guy, Int. J. Pharm. **271,** 251 (2004).
9. S. L. Raghavan, B. Kiepfer, A. F. Davis, S. G. Kazarian, and J. Hadgraft, Int. J. Pharm. **221,** 95 (2001).
10. M. Dias, J. Hadgraft, S. L. Raghavan, and J. Tetteh, J. Pharm. Sci. **93,** 186 (2004).
11. K. L. A. Chan and S. G. Kazarian, J. Biomed. Opt. **12,** 044010 0 (2007).
12. K. L. A. Chan and S. G. Kazarian, J. Comb. Chem. **7,** 185 (2005).
13. K. L. A. Chan and S. G. Kazarian, Lab Chip **6,** 864 (2006).
14. S. G. Kazarian, Anal. Bioanal. Chem. **388,** 529 (2007).
15. A. M. Kligman and E. Christophers, Arch. Dermatol. **88,** 702 (1963).
16. L. J. Chen, G. P. Lian, and L. J. Han, Ind. Eng. Chem. Res. **47,** 6465 (2008).
17. M. A. Pellett, A. C. Watkinson, J. Hadgraft, and K. R. Brain, Int. J. Pharm. **154,** 217 (1997).
18. W. J. Romonchuk and A. L. Bunge, J. Pharm. Sci. **95,** 2526 (2006).
19. E. M. Burka and R. Curbelo, US Patent 6141100, Imaging ATR spectrometer (2000).
20. S. G. Kazarian and K. L. A. Chan, Biochim. Biophys. Acta **1758,** 858 (2006).
21. S. G. Kazarian and J. Van der Weerd, Pharm. Res. **25,** 853 (2008).
22. A. J. Sommer, L. G. Tisinger, C. Marcott, and G. M. Story, Appl. Spectrosc. **55,** 252 (2001).
23. K. L. A. Chan and S. G. Kazarian, Analyst (Cambridge, U.K.) **131,** 126 (2006).
24. K. L. A. Chan and S. G. Kazarian, J. Comb. Chem. **8,** 26 (2006).
25. K. L. A. Chan and S. G. Kazarian, Appl. Spectrosc. **61,** 48 (2007).
26. W. J. McAuley, M. E. Lane, and J. Hadgraft, "ATR-FTIR spectroscopic investigation of the mechanisms by which DMSO enhances skin permeation", in *Annual Meeting of the American Association of Pharmaceutical Scientists* (Atlanta, GA, 2008).
27. C. W. Freudiger, W. Min, B. G. Saar, S. Lu, G. R. Holtom, C. He, J. C. Tsai, J. X. Kang, and S. Xie, Science (Washington, D.C.) **322,** 1857 (2008).